Expanding the Spectrum of FOXC1 and PITX2 Mutations and Copy Number Changes in Patients with Anterior Segment Malformations

D'haene, Barbara; Meire, Francoise; Claerhout, Ilse; Kroes, Hester Y.; Plomp, Astrid; Arens, Yvonne H.; de Ravel, Thomy; Casteels, Ingele; De Jaegere, Sarah; Hooghe, Sally

Published in:
Investigative ophthalmology & visual science

DOI:
10.1167/iovs.10-5309

Expanding the Spectrum of *FOXC1* and *PITX2* Mutations and Copy Number Changes in Patients with Anterior Segment Malformations

Barbara D'haene,[1] *Françoise Meire,*[2] *Ilse Claerhout,*[3] *Hester Y. Kroes,*[4] *Astrid Plomp,*[5,6] *Yvonne H. Arens,*[7] *Thomy de Ravel,*[8] *Ingele Casteels,*[9] *Sarah De Jaegere,*[1] *Sally Hooghe,*[1] *Wim Wuyts,*[10] *Jenneke van den Ende,*[10] *Françoise Roulez,*[11] *Hermine E. Veenstra-Knol,*[12] *Rogier A. Oldenburg,*[13] *Jacques Giltay,*[4] *Johanna B. G. M. Verheij,*[11] *Jan-Tjeerd de Faber,*[14] *Björn Menten,*[1] *Anne De Paepe,*[1] *Philippe Kestelyn,*[3] *Bart P. Leroy,*[1,3] *and Elfride De Baere*[1]

Purpose. Anterior segment dysgenesis (ASD) comprises a heterogeneous group of developmental abnormalities that affect several structures of the anterior segment of the eye. The main purpose of this study was to assess the proportion of *FOXC1* and *PITX2* mutations and copy number changes in 80 probands with ASD.

Methods. The patients were examined for *FOXC1* and *PITX2* copy number changes and mutations using MLPA (multiplex ligation-dependent probe amplification) and direct sequencing. Subsequently, the identified copy number changes were fine-mapped using high-resolution microarrays. In the remaining mutation-negative patients, sequencing of the *FOXC1* and-*PITX2* 3′ untranslated regions (UTRs) and three other candidate genes (*P32*, *PDP2*, and *FOXC2*) was performed.

Results. Thirteen *FOXC1* and eight *PITX2* mutations were identified, accounting for 26% (21/80) of the cases. In addition, six *FOXC1* and five *PITX2* deletions were found, explaining 14% (11/80) of the cases. The smallest *FOXC1* and *PITX2* deletions were 5.4 and 1.6 kb in size, respectively. Six patients carrying *FOXC1* deletions presented with variable extraocular phenotypic features such as hearing defects (in 4/6) and mental retardation (in 2/6). No further genetic defects were found in the remaining mutation-negative patients.

Conclusions. *FOXC1* and *PITX2* genetic defects explain 40% of our large ASD cohort. The current spectrum of intragenic *FOXC1* and *PITX2* mutations was extended considerably, the identified copy number changes were fine mapped, the smallest *FOXC1* and *PITX2* deletions reported so far were identified, and the need for dedicated copy number screening of the *FOXC1* and *PITX2* genomic landscape was emphasized. This study is unique in that sequence and copy number changes were screened simultaneously in both genes. (*Invest Ophthalmol Vis Sci.* 2011;52:324–333) DOI:10.1167/iovs.10-5309

From the [1]Center for Medical Genetics and the [3]Department of Ophthalmology, Ghent University Hospital, Ghent, Belgium; [2]Department of Ophthalmology, Queen Fabiola Children's University Hospital, Brussels, Belgium; the [4]Department of Medical Genetics, University Medical Center Utrecht, Utrecht, The Netherlands; the [5]Department of Clinical Genetics, Amsterdam Medical Center, Amsterdam, The Netherlands; the [6]Department of Clinical and Molecular Ophthalmogenetics, Netherlands Institute for Neuroscience, Royal Netherlands Academy of Arts and Sciences, Amsterdam, The Netherlands; the [7]Department of Clinical Genetics, University Hospital Maastricht, Maastricht, The Netherlands; the [8]Center for Human Genetics, University Hospitals Leuven, Leuven, Belgium; the [9]Department of Ophthalmology, University Hospitals Leuven-St.-Rafael, Leuven, Belgium; the [10]Department of Medical Genetics, University of Antwerp and University Hospital of Antwerp, Antwerp, Belgium; the [11]HUDERF (Hôpital Universitaire Des Enfants Reine Fabiola) Ophthalmology Department, Brussels, Belgium; the [12]Department of Genetics, University Medical Center Groningen, Groningen, The Netherlands; the [13]Department of Clinical Genetics, Erasmus MC Rotterdam, Rotterdam, The Netherlands; and the [14]Department of Ophthalmology, The Rotterdam Eye Hospital, Rotterdam, The Netherlands.

Supported by Specialisatiebeurs from Institute for the Promotion of Innovation through Science and Technology in Flanders (IWT-Vlaanderen) and Funds for Research in Ophthalmology (FRO) (BD). EDB is a senior clinical investigator of the Fund for Scientific Research (FWO).

Submitted for publication February 2, 2010; revised June 7, 2010; accepted July 6, 2010.

Disclosure: **B. D'haene**, None; **F. Meire**, None; **I. Claerhout**, None; **H.Y. Kroes**, None; **A. Plomp**, None; **Y.H. Arens**, None; **T. de Ravel**, None; **I. Casteels**, None; **S. De Jaegere**, None; **S. Hooghe**, None; **W. Wuyts**, None; **J. van den Ende**, None; **F. Roulez**, None; **H.E. Veenstra-Knol**, None; **R.A. Oldenburg**, None; **J. Giltay**, None; **J.B.G.M. Verheij**, None; **J.-T. de Faber**, None; **B. Menten**, None; **A. De Paepe**, None; **P. Kestelyn**, None; **B.P. Leroy**, None; **E. De Baere**, None

Corresponding author: Elfride De Baere, Center for Medical Genetics, Ghent University Hospital, De Pintelaan 185, B-9000 Ghent, Belgium; elfride.debaere@ugent.be.

Anterior segment dysgenesis (ASD) comprises a heterogeneous group of developmental abnormalities affecting several structures of the anterior segment of the eye. There are numerous classifications, largely based on clinical features, that generally fail to take into account either the embryologic derivatives of the affected structures or the underlying genetic defect.[1] Such clinical classification systems are hampered by the variability in clinical manifestations and by overlapping features between the subgroups.[1–3] As the underlying molecular genetics of the different subgroups are being unraveled, it becomes even more difficult.

Axenfeld-Rieger malformations (ARMs) represent a subgroup of ASD and refer to a group of autosomal dominant inherited disorders, affecting structures in the anterior eye segment derived from the neural crest. Apart from the classic ocular features, such as abnormal angle tissue, a hypoplastic or malformed iris, multiple pupils (polycoria), an elongated pupil (corectopia), and/or a posterior embryotoxon, ARM is often associated with systemic defects including dental, facial, and/or periumbilical abnormalities.[1,4] The major disease burden, however, brings with it the high risk of glaucoma, which develops in approximately 50% of ARM patients, potentially leading to visual loss or even blindness.[1,4] ARM is genetically

heterogeneous and has been associated with mutations in at least two transcription factor–encoding genes (*FOXC1*, *PITX2*) and with two known additional genetic loci (13q14, 16q24).[5–8] The association between ARM and *PAX6* in a patient with Rieger syndrome has been revised recently and appears to be incorrect.[9,10] It has been postulated that disease-causing mutations and copy number changes in *FOXC1* and *PITX2* account for less than 40% of the patients with ARM. However, this estimation should be interpreted with care, as it is based on studies involving small cohorts. Moreover, most studies did not include copy number analysis, which may have led to an underestimation of the contribution of *FOXC1* and *PITX2* in the molecular pathogenesis of ARM (reviewed in Ref. 4 and references therein). To date, 46 intragenic *FOXC1* and 41 intragenic *PITX2* mutations have been described, reflecting substantial allelic heterogeneity.[4] In addition, several chromosomal rearrangements and copy number changes have been described in the *FOXC1* and *PITX2* genomic landscape (Ref. 11 and references therein and Refs. 12–15). Both *FOXC1* gene deletions and duplications have been associated with ARM, underlining the need for a correct gene dosage for normal development of the anterior eye segment.[16,17]

In 2006, *FOXC1* and *PITX2* were shown to be co-expressed in the periocular mesenchyme.[18] Moreover, biochemical and subcellular localization assays demonstrated that these proteins physically interact with each other in a common complex on the chromatin. Apparently, PITX2 negatively regulates the functional activity of FOXC1, and, furthermore, functional assays have shown that PITX2 loss-of-function mutants lose their ability to inhibit FOXC1.[18] Additional studies designed to identify and define other members of the PITX2 and FOXC1 molecular pathways are critical in shaping our understanding of the molecular pathogenesis of ARM and in identifying novel candidate genes. Several co-expressed genes, direct protein interaction partners, upstream transcriptional regulators, and downstream transcriptional targets have been identified, such as P32, PDP2, and FOXC2.[19–24] The splicing factor SF2-associated protein (P32), for example, was isolated as a putative FOXC1-interacting protein by using a human trabecular meshwork (HTM) yeast two-hybrid (Y2H) cDNA library assay.[23] Huang et al.[23] demonstrated that this multicompartmental and multifunctional protein inhibits FOXC1 mediated transcriptional activation in a dose-dependent manner. Moreover, an impaired interaction was noted between the mutant FOXC1 protein p.Phe112Ser and P32. The pyruvate dehydrogenase phosphatase 2 gene (*PDP2*), in turn, was identified as a direct downstream target of PITX2 in a hormone-inducible *PITX2* expression system in nonpigmented ciliary body cells (NPCE) (Strungaru MH et al. *IOVS* 2007;48:ARVO E-Abstract 3212). *PDP2* encodes an enzyme from the pyruvate dehydrogenase complex (PDC), which is implicated in pyruvate decarboxylation within the mitochondria. FOXC2 is also thought to be involved in the FOXC1 pathway, as *FOXC1* and *FOXC2* show coordinated function and are co-expressed in the mesenchyme from which the ocular drainage structures are derived.[24]

The primary purpose of this study was to assess the prevalence of disease-causing *FOXC1* and *PITX2* mutations and copy number changes in a large cohort of 80 probands with ASD, mainly of Belgian-Dutch origin. Moreover, we sought to further characterize the identified copy number changes using high-resolution targeted microarrays, to assess the potential correlation between the extent of the deletions and disease severity.

In patients without coding *FOXC1/PITX2* intragenic mutations or copy number changes we sequenced the 3′UTRs, as these may harbor important regulatory pathogenic or modifying variants. In addition, genes encoding proteins involved in the same pathways as FOXC1 and PITX2, were considered to be plausible candidate genes in the remaining patients. To this end, we explored the putative involvement of three such candidate genes, *P32*, *PDP2*, and *FOXC2*, in the molecular pathogenesis of ASD.

Methods

Patients

The cohort consists of 80 diagnostic referrals for ARM derived from different ophthalmology clinics and genetics centers. More than 60% of the cohort originates from Belgium or the Netherlands. The study complied with the guidelines set forth in the Declaration of Helsinki.

The clinical records were reinspected for those patients in whom we identified a molecular defect involving *FOXC1* or *PITX2*. Of the 32 mutation-positive patients 12 (37.5%) were examined locally.

Direct Sequencing of *PITX2a*, *FOXC1*, *P32*, *FOXC2*, and *PDP2*

Primers were designed or selected from the literature to amplify the coding exons and intronic splice site junctions of *PITX2a* (NM_153427.1), *FOXC1* (NM_001453.2), *P32* (NM_001212.3), *PDP2* (NM_020786.1), and *FOXC2* (NM_005251.2) (primers available on request). *PITX2* consists of seven exons and can give rise to four alternative transcripts (*PITX2A*, *B*, *C*, and *D*).[25] We sequenced the coding region of *PITX2A*. In addition, primers were designed to generate overlapping amplicons covering the 3′UTR of *FOXC1* and *PITX2* (primers available on request). PCR products were sequenced in both directions with dye-termination chemistry (BigDye ver. 3.1 terminator cycle sequencing kit; Applied Biosystems, Inc. [ABI], Foster City, CA). Sequencing reactions were loaded on a genetic analyzer (model 3100 or 3730 with Sequencing Analysis ver. 3.7 and SeqScape ver. 1.1; ABI). *PITX2a* and *FOXC1* were sequenced in all patients. The amplicons in which we identified amino acid–altering variants were sequenced in 100 control samples to evaluate their significance. The 3′UTRs were sequenced in 40 patients negative for coding *FOXC1/PITX2* mutations or copy number changes. The remaining patients were not screened for the 3′UTRs because of a lack of sufficient DNA. Downstream screening of *P32*, *PDP2*, and *FOXC2* was performed for a pilot group of 31 probands without identifiable *FOXC1/PITX2* changes.

Sequence Variation Evaluation and Nomenclature of Mutations

The presence of all mutations was confirmed on a second PCR product. Segregation analysis of disease alleles was performed if possible. Thorough bioinformatic evaluation of novel variants was performed (Alamut software, ver.1.5; Interactive Tiosoftware, Rouen, France). Alamut provides for each variant the HGVS (Human Genome Variation Society, Genomic Disorders Research Centre, Carlton South, VIC Australia) nomenclature. For missense variants, it calculates the Grantham distance and automatically fills in the queries for PolyPhen and SIFT prediction servers, based on the UniProt[26] protein identifiers and FASTA sequences of several orthologs, respectively (Polyphen, http://genetics.bwh.harvard.edu/pph/ provided in the public domain by the Division of Genetics, Department of Medicine, Brigham and Women's Hospital, Harvard Medical School, Boston, MA, and the Bork Group, EMBL, Heidelberg, Germany; SIFT [sorting tolerant from intolerant], http://www.fhcrc.org/ provided in the public domain by the Fred Hutchinson Cancer Research Center, Seattle, WA; FASTA, http://www.ebi.ac.uk/tools/fasta/ provided in the public domain by the European Bioinformatics Institute, European Molecular Biology Laboratory, Heidelberg, Germany). Variants with a major impact on protein level—for example, through the introduction of stop codons, frame shifts or large deletions, duplications or insertions—were classified as pathogenic. Variants within the 3′UTR that were not registered as a known SNP in the Ensembl Genome Browser[27] were classified as putative pathogenic. The numbering of DNA sequence variants was performed according to the HGVS Mutation Nomenclature Recommendations

TABLE 1. Summary of Identified *FOXC1* and *PITX2* Mutations with Associated Phenotypes

Mutation (cDNA)	Mutation (Protein)	Protein Domain	YOB; Sex	Type; Segregation	Ocular Features	Extraocular Features
FOXC1						
c.286dupG	p.Asp96GlyfsX210	FHD	1973; F	S; Mother − Father/	Bilateral glaucoma, bilateral posterior embryotoxon and angle abnormalities, cataract and corneal opacities in right eye	None reported
c.316C>T	**p.Gln106X**	FHD	1985; M	S; Mother/Father/	Enucleation of the right eye due to severe glaucoma. Left eye: posterior embryotoxon, hazy peripheral cornea, limited ectropion uveae at pupillary border, limited iris hypop lasia, anterior synechiae	None reported
c.325A>G	**p.Met109Val**	FHD	1978; M	?; Mother − Father +	Unilateral corectopia, blue sclerae	Maxillary hypoplasia, dental anomalies, hearing loss, learning difficulties
c.335del	**p.Phe112SerfsX69**	FHD	1983; F	F; Mother + Father/	Bilateral glaucoma and buphthalmos, Rieger anomaly	Mild dental anomalies, unilateral hearing impairment
c.392C>A	**p.Ser131X**	FHD	1978; M	F; Mother + Father − Brother −	Bilateral glaucoma, left eye enucleated	Dental anomalies, epilepsy
c.392C>G	**p.Ser131Trp**	FHD	1984; F	?; Mother/Father/	Iris hypoplasia, Rieger anomaly	Congenital scoliosis, dental anomalies
c.412A>G	**p.Lys138Glu**	FHD	1975; M	?; Mother/Father/	Normal tension glaucoma, clear cornea, clear lens, posterior embryotoxon	None reported
c.605delC	**p.Pro202ArgfsX113**		2001; F	F; Mother + Father − Brother +	Unilateral glaucoma, unilateral Haab's striae, (mild iris hypoplasia), unilateral posterior embryotoxon	Maxillary hypoplasia anomaly, hypertelorism
c.692_696del	**p.Gly231ValfsX73**	ID	1995; F	S; Mother − Father +	Glaucoma, Axenfeld-Rieger anomaly, no other data obtained	No data obtained
c.780dup	**p.Asp261ArgfsX45**	ID	?; M	F; Mother + Father/	No data obtained	No data obtained
c.816_817delinsG	**p.Ser272ArgfsX43**	ID	1979; M	S; Mother − Father −	No data obtained	No data obtained
c.980_981del	**p.Glu327AlafsX200**	ID	1977; F	?; Mother/Father/	No data obtained	No data obtained
c.1491C>G	**p.Tyr497X**	AD2	2006; M	F; Mother/Father +	Glaucoma, no other data obtained	Hypertelorism
PITX2						
c.137_138del	**p.Phe46TyrfsX152**	HD	2002; M	S; Mother − Father/	Unilateral glaucoma, bilateral posterior embryotoxon, bilateral polycoria, corectopia, anterior synechiae, bilateral angle abnormalities	Maxillary hypoplasi a, umbilical anomaly, dental anomalies
c.172T>C	**p.Phe58Leu**	HD	1994; M	S; Mother − Father −	Bilateral glaucoma, irregular pupil, anterior synechiae	Maxillary hypoplasia, umbilical anomaly, dental anomalies, tachycardia, hyperextension of elbow and finger joints, history of multiple sprained ankles, fifth finger clinodactyly and brachymesophalangia
c.175C>T	**p.Gln59X**	HD	?; M	S; Mother − Father −	Rieger syndrome, no other data obtained	No data obtained
c.224G>A	**p.Trp75X**	HD	1999; M	S; Mother − Father −	Unilateral glaucoma, bilateral posterior embryotoxon, bilateral corectopia	Maxillary hypoplasia, umbilical anomaly, dental anomalies, bilateral retention of th e testis
c.253–11A>G	/	/	1998; M	F; Mother + Father/ Sister: +	Unilateral posterior embryotoxon, bilateral corectopia, pigmentation on anterior lens capsule	Maxillary hypoplasia, umbilical anomaly, dental anomalies, short stature

(*continues*)

TABLE 1 (*continued*). Summary of Identified *FOXC1* and *PITX2* Mutations with Associated Phenotypes

Mutation (cDNA)	Mutation (Protein)	Protein Domain	YOB; Sex	Type; Segregation	Ocular Features	Extraocular Features
c.282G>A	p.Trp94X	HD	1994; M	F; Mother + Father − Sister: +	Severe iridocorneal dysgenesis with corneal endothelium decompensation and edema, unilateral corectopia	Maxillary hypoplasia, dental anomalies, umbilicus not examined, hear ing loss, hypertelorism, speech and language delay, motor retardation, short palatum
c.301C>T	**p.Gln101X**	ID1	2003; F	S; Mother − Father −	No glaucoma, Right eye: leucoma and eccentric irregular pupil. Left eye: transparent cornea, polycoria	Maxillary hypoplasia, umbilical anomaly, dental anomal ies
c.304C>T	**p.Gln102X**	ID1	1981; F	S; Mother/Father/	No data obtained	Redundant umbilical skin, dental anomalies

Novel mutations are shown in bold. YOB, year of birth; F, familial; S, sporadic; +, positive for the mutation; −, negative for the mutation;/, not available for testing.

(http://www.hgvs.org/mutnomen/recs.html/ provided in the public domain by the Human Genome Variation Society). The *FOXC1* mutations are described according to RefSeq: NM_001453.2. The *PITX2* mutations are described according to the *PITX2* transcript variant 1 (RefSeq: NM_153427.1) (www.ncbi.nlm.nih.gov/locuslink/refseq/ provided in the public domain by the National Center for Biotechnology Information, Bethesda, MD).

Multiplex Ligation-Dependent Probe Amplification

MLPA permits relative quantification of changes in copy number of specific genomic regions.[28] The P054 probe mix includes probes for the *TWIST1*, *FOXL2*, *FOXC1*, *FOXC2*, *ATR*, *PITX2*, and *OA1* genes. More specifically, it contains three probes for *PITX2*, two probes for *FOXC1*, and two probes for *FOXC2*. MLPA was performed in accordance with the manufacturer's instructions (MRC Holland; Amsterdam, The Netherlands).

Copy Number Analysis Using 250K SNP Arrays

Three *PITX2* deletions identified using MLPA were subsequently delineated using 250K *Nsp*I SNP arrays (Affymetrix, Santa Clara, CA). Processing of the samples, quality control, and SNP copy number assessment was conducted by an Affymetrix Service Provider (CNAT 4.0 software; DNA Vision, Charleroi, Belgium). The results were subsequently visualized in arrayCGHbase.[29]

Copy Number Analysis with Targeted High-Resolution Arrays

During the study, it became possible to design a custom-targeted 60K oligonucleotide (Agilent Technologies, Palo Alto, CA) targeting a region of 5 Mb around *FOXC1* (chr6:1–5000000; UCSC, Human Genome Browser, March 2006/ provided by the University of California Santa Cruz at http://genome.ucsc.edu) and a region of 5 Mb around *PITX2* (chr4:109258234-114257994; UCSC, Human Genome Browser, March 2006). Using this array, we characterized four *FOXC1* deletions, two partial *FOXC1* deletions, one *PITX2* deletion, and one partial *PITX2* deletion, originally identified through MLPA.

Hybridizations were performed according to the manufacturer's instructions, with minor modifications.[30] The results were subsequently visualized in arrayCGHbase.[29]

RESULTS

FOXC1 and *PITX2* Screening

Molecular screening of *FOXC1* and *PITX2* in 80 probands with ASD resulted in the identification of mutations in 32 (40%) of 80 patients. In particular, an *FOXC1* mutation/copy number change was detected in 19 (24%) patients, and a *PITX2* mutation/copy number change was detected in 13 (16%) patients. The mutations are listed in Table 1 with novel mutations represented in bold. Copy number changes are listed in Table 2.

In *FOXC1* we identified 13 mutations in 13 unrelated probands: 3 nonsense, 7 frameshift, and 3 missense mutations (Table 1, Fig. 1). To the best of our knowledge, 12 of 13 are novel. In general, nonsense and frameshift mutations were considered to be pathogenic. The effect of three missense mutations (p.Met109Val, p.Ser131Trp, and p.Lys138Glu) on protein function was more difficult to assess, and computational programs were used to predict their pathogenic character (Supplementary Material S1, http://www.iovs.org/lookup/suppl/doi:10.1167/iovs.10-5309/-/DCSupplemental). All three mutations are located within the highly conserved DNA-binding forkhead domain (Supplementary Material S2, http://www.iovs.org/lookup/suppl/doi:10.1167/iovs.10-5309/-/DCSupplemental) and probably affect the DNA-binding capacity. Although the compu-

TABLE 2. Summary of Identified *FOXC1* and *PITX2* Deletions with Associated Phenotype types

Deletion	Max Size; Position (chr6)*	YOB; Sex	Type; Segregation	Ocular Features	Extraocular Features
FOXC1					
*FOXC1*_1	~5.4 kb; 1553924–1559364	2003; M	S; Mother − Father −	No glaucoma, megalocornea, bilateral posterior embryotoxon	Hypertelorism, maxillary hypoplasia, no cardiac anomaly, no growth retardation, no umbilic al anomaly, no dental anomalies
*FOXC1*_2	~34 kb; 1551415–1585522	1973; F	F; Mother + Father/ Children: −	Right eye: glaucoma, posterior embryotoxon, megalocornea, Haab's striae, corectopia, iris strands, ectropion uveae Left eye: glaucoma, megalocornea, Haab's striae, corectopia, iris strands, polycoria, nuclear cataract	Hypertelorism, maxillary hypop lasia, progressive hearing loss, no umbilical anomaly, no dental anomalies, normal intelligence
*FOXC1*_3	~84 kb; 1552945–1636775	1982; F	F; Mother − Father −	Bilateral glaucoma, posterior embryotoxon, atrophic iris	No data obtained
*FOXC1*_4	~2.6 Mb; 0–2646377	1966; M	F; Mother/Father/Brother +	Glaucoma, Descemet membrane ruptures, limited peripheral cornea nebulae Right eye: corticonuclear cataract, iris hypoplasia, upward pupillary displacement, anterior synechiae Left eye: discrete anterior subcapsular cataract, iris hypoplasia, polycoria	Maxillary hypoplasia, hearing loss due to middle ear malformations, tooth extraction required because of maxillary dental crowding with normal number of teeth, no cardiac anomaly, no umbilical anomaly, normal intelligence
*FOXC1*_5	~3.4 Mb; 566884–3960186	1978; F	F; Mother/Father/	Right eye: glaucoma, partial posterior embryotoxon Left eye: glaucoma, partial posterior embryotoxon, anterior synechiae in area of cystic schisis of inferior iris	Mild mental retardation, middle ear hearing loss, eczema, no growth retardation, no umbilical anomaly
*FOXC1*_6	~4.7 Mb; 0–4749872	1994; F	S; Mother + Father/ Brother −	Bilateral irregular pupil, iridocorneal adhesions, prominent Schwalbe's line	Minor maxillary hypoplasia, no cardiac anomaly, no growth retardation, no umbilical anomaly, dental anomalies, small mouth, small nose, chronic glue ear and hearing loss, hyperlax long fingers, IQ 56 with developmental and speech delay, premature pubarche and axillarche
PITX2					
*PITX2*_1	1.6 kb; 111760308–111761945	2006; M	S; Mother − Father −	Unilateral microcornea	Maxillary hypoplasia, umbilical anomaly, dental anomalies, no cardiac anomalies, no growth retardation
*PITX2*_2	286 kb; 111648252–111934227	2008; F	S; Mother − Father −	Right eye: mild atrophic iris Left eye: corectopia, atrophic iris, iridocorneal adhesions	Maxillary hypoplasia, umbilical anomaly, dental anomalies, normal intelligence, no cardiac/renal anomalies, no growth ret ardation
*PITX2*_3	~1.1 Mb; 111161726–112223083	?; M	F; Mother/Father/	Bilateral glaucoma, bilateral posterior embryotoxon, unilateral polycoria, bilateral corectopia	Maxillary hypoplasia, umbilical anomaly, dental anomalies, normal intelligence, no cardiac anomalies, no growth retardation
*PITX2*_4	~2.5 Mb; 110200973–112725989	1960; M	S; Mother/Father/	Severe bilateral glaucoma, anterior segment anomalies. No other data	Umbilical anomaly, dental anomalies, normal intelligence
*PITX2*_5	~2.8 Mb; 110322934–113076304	1974; M	S; Mother/Father/	No glaucoma, asymmetric ocular anomalies Right eye: posterior embryotoxon, dyscoria, Fuchs endothelial dystrophy Left eye: polycoria, corectopia, anterior synechiae	Umbilical anomaly, dental anomalies, no cardiac anomaly, intelligence not specified

YOB, year of birth; F, familial; S, sporadic; +, positive for the mutation; −, negative for the mutation;/, not available for testing.

* Chromosomal position according to the UCSC, Human Genome Browser, March 2006.

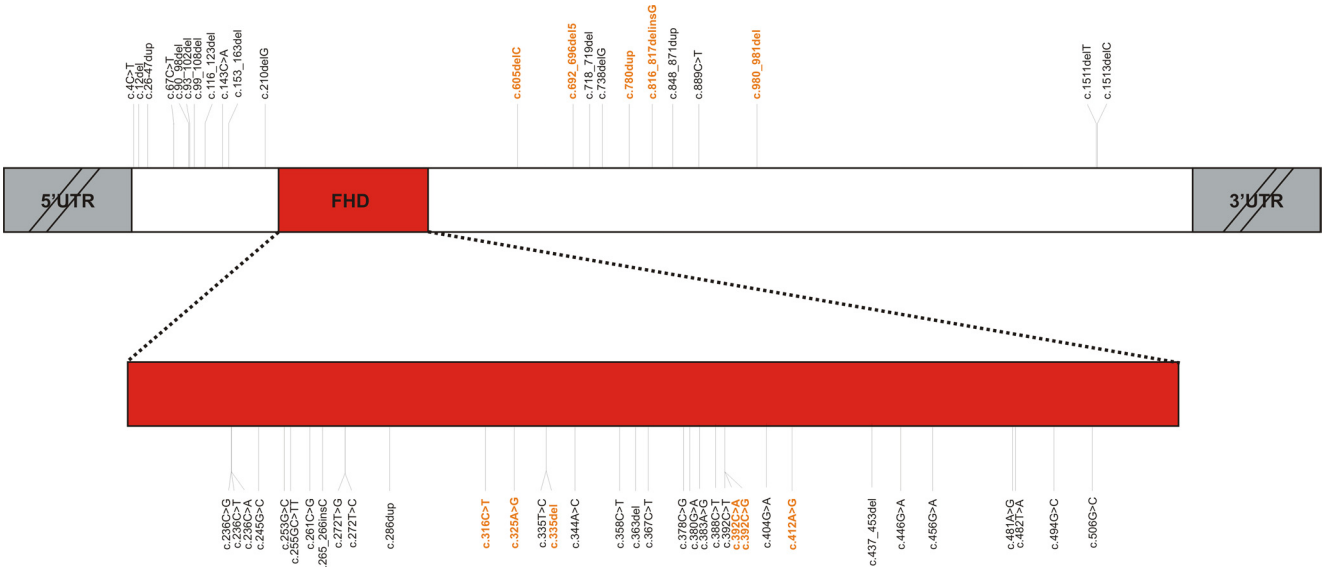

FIGURE 1. Overview of all known and novel *FOXC1* mutations. Shown (drawn to scale) is the *FOXC1* coding region, with all known (*black lettering*) and novel (*orange lettering*) *FOXC1* mutations. *Red*: The DNA-binding FHD. *Gray*: The 5′ and 3′ UTRs (not drawn to scale).

tational predictions sometimes contradict each other, all three substitutions were regarded as pathogenic because of their location in the highly conserved forkhead domain (Supplementary Material S2, http://www.iovs.org/lookup/suppl/doi:10.1167/iovs.10-5309/-/DCSupplemental), the overall outcome of the different programs and the Grantham score (Supplementary Material S1, http://www.iovs.org/lookup/suppl/doi:10.1167/iovs.10-5309/-/DCSupplemental), and their absence in the 100 control samples. Sequence analysis of the *FOXC1* 3′UTR of 40 patients in whom no pathogenic mutation was identified in the *FOXC1* coding region, led to the identification of several registered SNPs, but no putative pathogenic variants were found. Furthermore, we identified

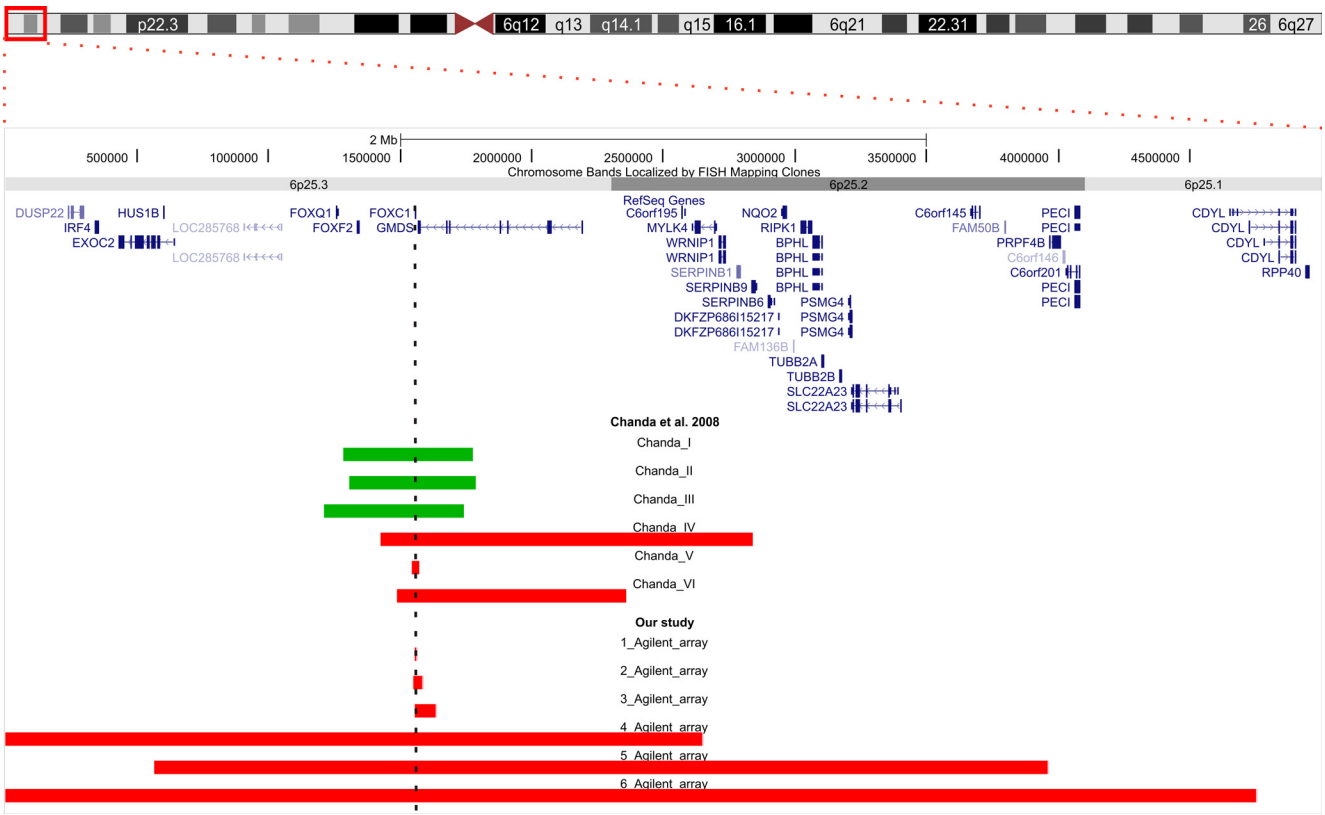

FIGURE 2. Overview of delineated *FOXC1* deletions. The *FOXC1* region with custom tracks showing the extent of the molecularly defined deletions reported by Chanda et al.[12] and identified in the current study. *Horizontal red bars*: locations and sizes of deletions; *horizontal green bars*: locations and sizes of duplications. (Drawn according to the UCSC, Human Genome Browser, March 2006; University of California Santa Cruz.)

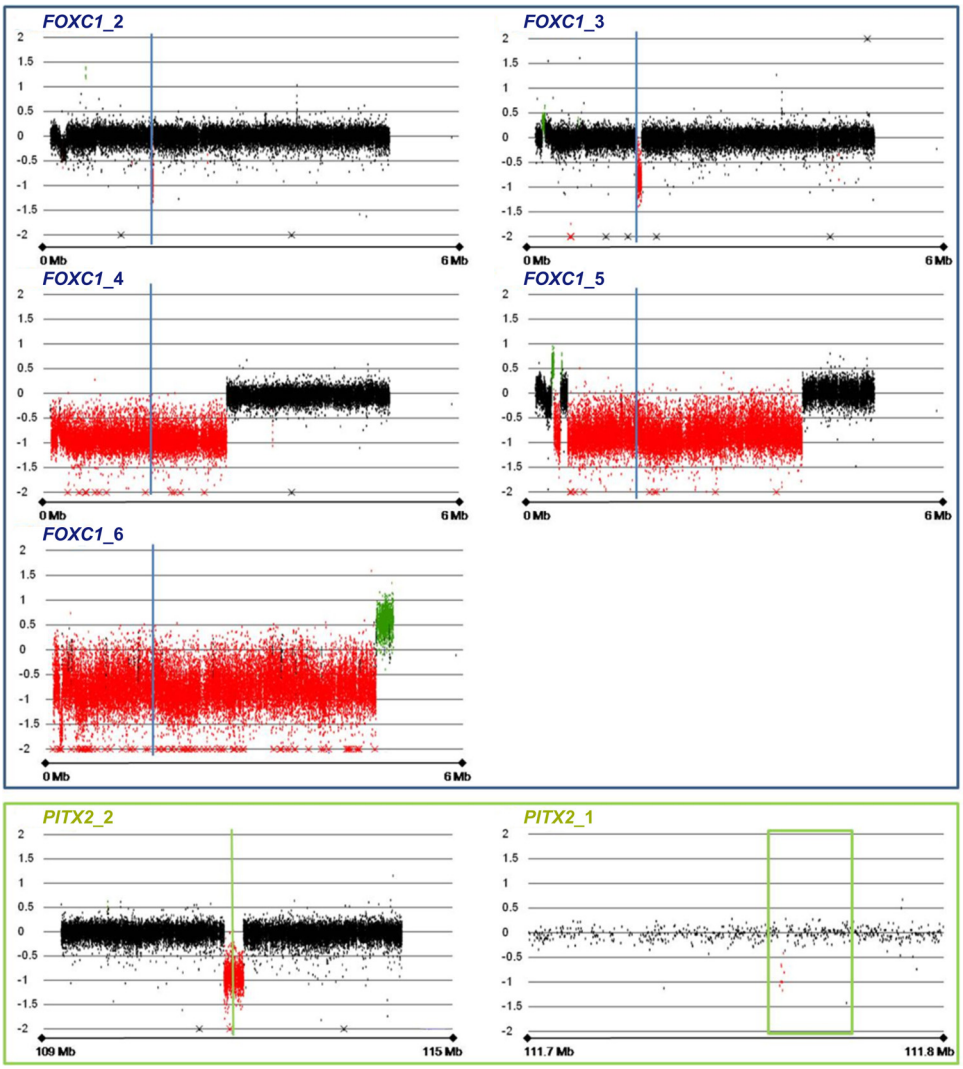

FIGURE 3. Copy number analysis by targeted arrays (Agilent; Palo Alto, CA). *Blue box*: array CGH profiles for the *FOXC1* region (chromosome [chr]6:0-6,000,000) showing five samples with *FOXC1* deletions. *Blue vertical line*: location of *FOXC1*. *Green box*: profiles for the *PITX2* region showing two samples with *PITX2* deletions. The location of *PITX2* are marked in the first (*green vertical line*) and second (*green rectangle*) profiles. *Colored dots*: $\log_2$ ratios of individual oligonucleotides (*red*: deleted; *black*: normal; *green*: duplicated).

two partial and four total *FOXC1* gene deletions with MLPA, which were further characterized by targeted microarray (Figs. 2, 3; Table 2). There was a scattered location of the breakpoint regions, and the deletions appeared to be at maximum 4.7 Mb, 3.4 Mb, 2.6 Mb, 84 kb, 34 kb, and 5.4 kb in size.

Within *PITX2*, we identified eight different mutations: five nonsense, one frameshift, one missense, and one splice site (Table 1; Fig. 4). Overall, six of eight mutations are novel. As for *FOXC1*, the nonsense and frameshift mutations identified in *PITX2* are believed to have a major effect on the protein function and, hence, were considered pathogenic. The missense mutation p.Phe58Leu is located within the evolutionarily conserved DNA-binding homeodomain (Supplementary Material S2, http://www.iovs.org/lookup/suppl/doi:10.1167/iovs.10-5309/-/DCSupplemental) and Polyphen and SIFT analysis assign this substitution as "possibly pathogenic" and "not tolerated," respectively (Supplementary Material S1, http://www.iovs.org/lookup/suppl/doi:10.1167/iovs.10-5309/-/DCSupplemental). Although the Grantham score suggests a minor impact, the overall results are in favor of a pathogenic character. Moreover, this variant is de novo, as it was not found in the DNA from both unaffected parents, and it was absent in 100 control samples. Sequence analysis of the *PITX2* 3′UTR revealed several known SNPs and one putative pathogenic variant, which was not registered as a known SNP, in a patient of Caucasian origin. However, the de novo character of this latter variant could not be assessed because of the lack of parental DNA. Furthermore, one partial and four total *PITX2* deletions were identified by MLPA. The partial deletion spanned one of four MLPA probes and appeared to be de novo. The *PITX2* deletions were further delineated with 250K SNP arrays (Affymetrix) or targeted 60K arrays (Agilent). This method enabled characterization of the extent of all five deletions (Fig. 5). The breakpoints were scattered and the maximum size of the deletions were 2.5 Mb, 2.8 Mb, 1.1 Mb, 286 kb, and 1.6 kb (Figs. 3, 5; Table 2).

The corresponding ocular and extraocular phenotypes of patients with established genotypes are provided in detail in Tables 1 and 2.

Sequencing Analysis of Selected Candidate Genes

Downstream screening of a pilot group of 31 probands without identifiable *FOXC1/PITX2* changes consisted of sequencing three candidate genes *P32*, *PDP2*, and *FOXC2*. Apart from known SNPs, we identified one sequence variant within *PDP2* (c.1083G>A, p.Arg361His). However, this variant was not classified as pathogenic, based on several in silico predictions. Polyphen predicted this variant to be benign, and according to SIFT predictions, the protein substitution is tolerated. In addition, the Grantham distance of this substitution was only 29. Because of the lack of pathogenic sequence variants in this

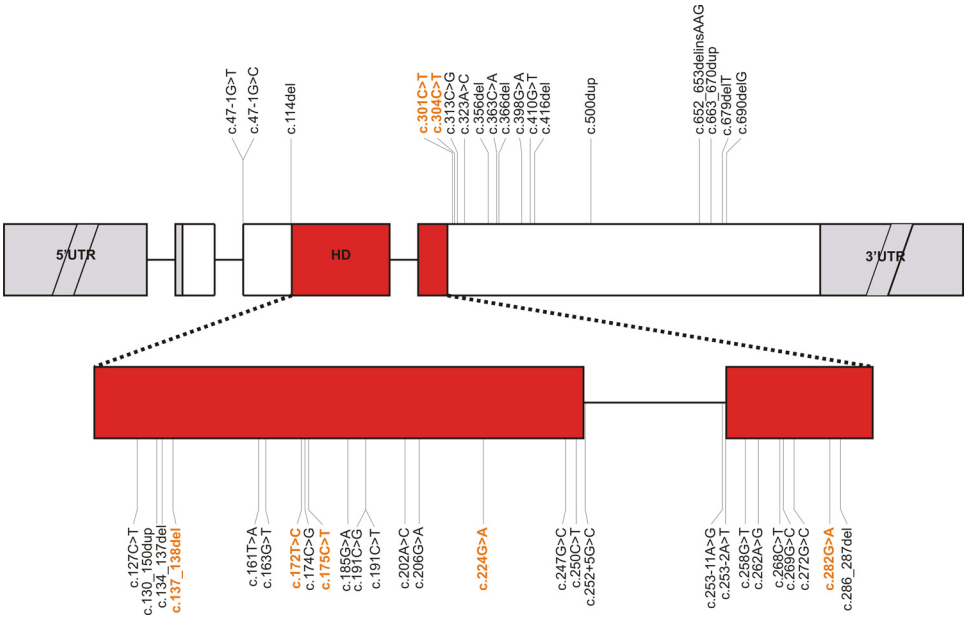

FIGURE 4. Overview of all known and novel *PITX2* mutations. A scale drawing of the *PITX2* coding region, with all known (*black lettering*) and all novel (*orange lettering*) *PITX2* mutations. *Red*: the DNA-binding homeodomain (HD). *Gray*: 5′ and 3′ UTRs (not drawn to scale). The exonic regions are represented by *boxes* and the separating intronic regions (not drawn to scale) are depicted by *horizontal lines* between two subsequent boxes.

pilot group of patients, we refrained from screening additional patients.

DISCUSSION

Molecular screening of *FOXC1* and *PITX2* in a large cohort (80 probands with ASD) led to the identification of the underlying molecular defect in 40% of the patients. This study is unique in that we simultaneously screened for sequence changes (coding region and 3′UTRs) and copy number changes in both genes. Twelve novel *FOXC1* and six novel *PITX2* mutations extend the spectrum of 46 and 41 reported intragenic *FOXC1* and *PITX2* mutations, respectively. Of note, most of the reported mutations in these two genes are unique, emphasizing their allelic heterogeneity.

The single-exon gene *FOXC1* is located on chromosome band 6p25 and encodes a forkhead transcription factor. It is a member of a gene family that is characterized by an evolutionarily conserved 110 amino acid (AA), DNA-binding forkhead domain (FHD). Apart from this FHD, FOXC1 contains a terminal protein sequence of unknown function that is conserved up to *Xenopus*.[2] We identified six novel mutations within and six novel mutations downstream of the FHD. When all known and novel *FOXC1* mutations were taken into account, missense

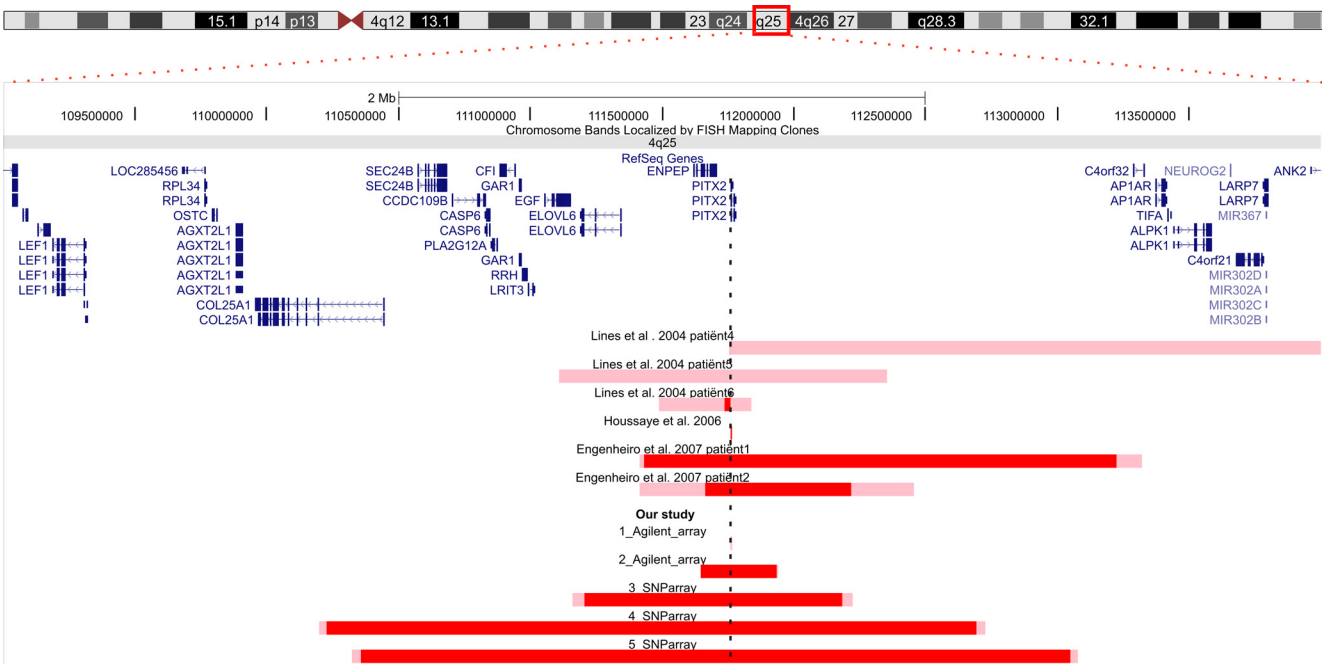

FIGURE 5. Overview of delineated *PITX2* deletions. The *PITX2* region (4q25–q26) with custom tracks showing the extent of all molecularly defined deletions reported in the literature[13–15] and in the present study. *Horizontal red bars*: locations and sizes of deletions. *Red*: minimally deleted regions; *pink*: regions harboring the breakpoints. (Drawn according to the UCSC, Human Genome Browser, March 2006; University of California Santa Cruz.)

mutations were the most common (45%), whereas frameshift mutations were overrepresented outside the FHD.

The *PITX2* gene, located on 4p25, encodes a member of the bicoid class of homeodomain (HD) proteins and was the first gene to be associated with ARM.[7] This gene consists of seven exons and can give rise to four alternative transcripts (*PITX2A*, *B*, *C*, and *D*).[25] The PITX2A protein, which is expressed in the developing eye, can be subdivided into five regions; two activation domains (AD), one homeodomain (HD), and two inhibitory domains (ID).[31] In general, frameshift and nonsense mutations in *PITX2* are scattered along the coding region, whereas most missense mutations are restricted to the DNA-binding HD. We identified five mutations that are presumed to affect the DNA-binding capacity of the HD severely. Furthermore, we identified two nonsense mutations within the ID1. The latter mutations left the HD intact, but completely ablated ID1, ID2, and AD2. Taking into account all known and novel *PITX2* mutations, missense mutations appeared to be the most prominent (45%). It is noteworthy that more than half of the mutations were located within the HD (62%).

Both *FOXC1* and *PITX2* mutations can be associated with a wide spectrum of anterior segment phenotypes that do not differ significantly. Moreover, there is inter- and intrafamilial variable expressivity for certain point mutations,[32,33] and mutations in either *FOXC1* or *PITX2* are prevalent in different clinical subgroups of the ASD spectrum (Supplementary Material S3, http://www.iovs.org/lookup/suppl/doi:10.1167/iovs.10-5309/-/DCSupplemental; Fig. 6).[6,34]

In this study, MLPA revealed six *FOXC1* and five *PITX2* deletions. The *FOXC1* deletions can be added to the relatively large number of chromosomal rearrangements involving 6p25, but only a handful of these have been accurately characterized at the molecular level[12,35] (as reviewed in Ref. 11). Recently, 10 duplications and deletions spanning *FOXC1* were delineated in detail using targeted oligonucleotide arrays and detailed junction analysis. These rearrangements were nonrecurrent and a spectrum of recombination, DNA repair and replication were presumed to underlie these 6p25 rearrangements.[12] In this study, we further assessed the extent of the deletions with a targeted microarray and compared their location and extent with those described by Chanda et al.[12] (Figs. 2, 6).

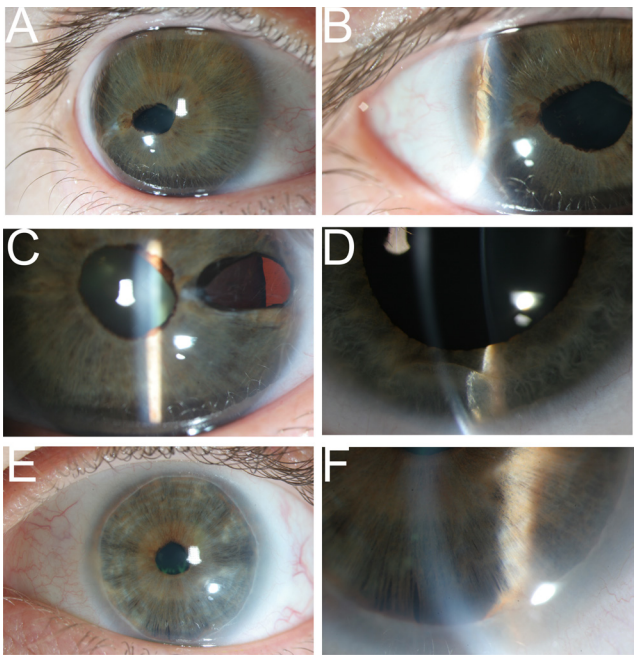

Figure 6. Anterior segment photographs from patients with *FOXC1* genetic defects. (**A–C**) Ocular images from a patient carrying a partial *FOXC1* deletion (*FOXC1_2*, Table 2). (**A**) Ectopic pupil and posterior embryotoxon in a right eye. (**B**) Iris strands in a right eye. (**C**) Peripheral polycoria and ectropion uveae in a left eye. (**D**) Anterior synechiae and iris cyst in the left eye from a patient carrying a relatively large *FOXC1* deletion (*FOXC1_5*, Table 2). (**E**, **F**) Ocular images of an eye of a patient with a *FOXC1* mutation c.316C>T (Table 1). (**E**) Image of the left eye showing posterior embryotoxon and limited iris hypoplasia. (**F**) Anterior synechiae in the left eye.

To date, only 14 microscopic or submicroscopic deletions spanning *PITX2* have been reported, and the extent of these was further defined at the molecular level in only 6 of 14 cases.[4,13–15] We delineated five *PITX2* deletions by using arrays and subsequently compared them with deletions described previously (Fig. 5). The location of the breakpoints is scattered, which is indicative of the absence of a recombination hotspot. Such nonrecurrent rearrangement events may be explained by nonhomologous end joining (NHEJ), alternative NHEJ (alt-NHEJ), fork stalling and template switching (FoSTeS), or variations on these models as possible underlying mechanisms.[12,36]

Of interest, there appeared to be no phenotypic differences between patients with intragenic *PITX2* mutations and *PITX2* deletions (Tables 1, 2). Furthermore, it should be noted that the patients carrying relatively large deletions had normal intelligence and did not display other obvious extraocular congenital malformations (Table 2). Based on the latter observation, we presume that no other dosage-sensitive genes are located in the *PITX2* neighboring region.

Our study not only provides substantial molecular and clinical data, but also demonstrates that deletions in the *FOXC1* and *PITX2* region can most easily be detected using MLPA with a commercially available probe mix. However, other techniques can be used to identify such copy number changes, including microsatellite analysis, quantitative PCR (qPCR), and copy number screening with microarrays. Microsatellite analysis has been successfully applied to identify *PITX2* copy number changes by Lines et al.,[15] but the major drawback for this is the need for parental DNA.[15] A better option is copy number screening using qPCR, which is flexible and comes at a relatively low average cost.[37] High-density (targeted or genomewide) oligonucleotide arrays may be regarded as the ultimate alternative to MLPA and qPCR, but these arrays are still relatively expensive and require more hands-on time. On the other hand, they allow the assessment of the extent of the copy number change. Finally, the use of genomewide microarrays may lead to the identification of novel candidate regions.

Recently, Tümer and Bach-Holm[4] generated a decision-tree aimed at selecting the most cost-effective diagnostic strategy for patients with a tentative diagnosis of ARM. However, in our diagnostic setting we perform direct sequencing of the open reading frames (ORFs) and MLPA in parallel. In our view, this is the most cost- and time-efficient strategy, leading to the identification of the underlying molecular defect in at least 40% of the diagnostic referrals for ARM.

The large proportion of molecularly unsolved ASD patients indicates the involvement of other genes in the molecular pathogenesis of anterior segment malformations. Hence, mutation screening of three plausible candidate genes (*P32, PDP2*, and *FOXC2*) was undertaken in a pilot group of molecularly unsolved patients, but did not reveal any pathogenic mutation. Future strategies toward disease gene identification may include massive parallel sequencing of a spectrum of genes involved in ocular development, or high-resolution genomewide microarray-based copy number profiling for the identification of disease causing copy number changes. The latter strategy was applied with success in Peters Plus syndrome, an autosomal recessive disorder characterized by ante-

rior eye chamber abnormalities, disproportionate short stature, and developmental delay.[38] To our knowledge, a systematic genomewide search for new copy number variations (CNVs) in ASD patients has not yet been performed, and might lead toward the identification of novel ASD disease genes.

In conclusion, there were underlying *FOXC1/PITX2* genetic defects in 40% of our large ASD cohort. We considerably extended the current spectrum of intragenic *FOXC1/PITX2* mutations and copy number changes, identified the smallest *FOXC1/PITX2* deletions reported so far, and emphasized the need for dedicated copy number screening of the *FOXC1* and *PITX2* genomic landscape in ASD. Finally, mutations in the 3′UTR of *FOXC1*and *PITX2*, and in the ORF of *P32*, *PDP2*, and *FOXC2* did not play a major role in the ASD cases examined in this study.

Acknowledgments

The authors thank the clinicians for providing patient samples and the families who participated in this study.

References

1. Idrees F, Vaideanu D, Fraser SG, Sowden JC, Khaw PT. A review of anterior segment dysgeneses. *Surv Ophthalmol.* 2006;51:213–231.
2. Hjalt TA, Semina EV. Current molecular understanding of Axenfeld-Rieger syndrome. *Expert Rev Mol Med.* 2005;7:1–17.
3. Amendt BA, Semina EV, Alward WL. Rieger syndrome: a clinical, molecular, and biochemical analysis. *Cell Mol Life Sci.* 2000;57:1652–1666.
4. Tümer Z, Bach-Holm D. Axenfeld-Rieger syndrome and spectrum of PITX2 and FOXC1 mutations. *Eur J Hum Genet.* 2009;17:1527–1539.
5. Werner W, Kraft S, Callen DF, Bartsch O, Hinkel GK. A small deletion of 16q23.1→[del(16)(q23.1q24.2).ish del(16)(q23.1q24.2)(D16S395+, D16S348−, P5432+)] in a boy with iris coloboma and minor anomalies. *Am J Med Genet.* 1997;70:371–376.
6. Mirzayans F, Gould DB, Heon E, et al. Axenfeld-Rieger syndrome resulting from mutation of the FKHL7 gene on chromosome 6p25. *Eur J Hum Genet.* 2000;8:71–74.
7. Semina EV, Reiter R, Leysens NJ, et al. Cloning and characterization of a novel bicoid-related homeobox transcription factor gene, RIEG, involved in Rieger syndrome. *Nat Genet.* 1996;14:392–399.
8. Phillips JC, del Bono EA, Haines JL, et al. A second locus for Rieger syndrome maps to chromosome 13q14. *Am J Hum Genet.* 1996;59:613–619.
9. Riise R, Storhaug K, Brondum-Nielsen K. Rieger syndrome is associated with PAX6 deletion. *Acta Ophthalmol Scand.* 2001;79:201–203.
10. Riise R, D'Haene B, De Baere E, Gronskov K, Brondum-Nielsen K. Rieger syndrome is not associated with PAX6 deletion: a correction to *Acta Ophthalmol Scand*. 2001: 79: 201–203. *Acta Ophthalmol.* 2009;87:923.
11. Gould DB, Jaafar MS, Addison MK, et al. Phenotypic and molecular assessment of seven patients with 6p25 deletion syndrome: relevance to ocular dysgenesis and hearing impairment. *BMC Med Genet.* 2004;5:17.
12. Chanda B, Asai-Coakwell M, Ye M, et al. A novel mechanistic spectrum underlies glaucoma-associated chromosome 6p25 copy number variation. *Hum Mol Genet.* 2008;17:3446–3458.
13. Engenheiro E, Saraiva J, Carreira I, et al. Cytogenetically invisible microdeletions involving PITX2 in Rieger syndrome. *Clin Genet.* 2007;72:464–470.
14. de la Houssaye G, Bieche I, Roche O, et al. Identification of the first intragenic deletion of the PITX2 gene causing an Axenfeld-Rieger syndrome: case report. *BMC Med Genet.* 2006;7:82.
15. Lines MA, Kozlowski K, Kulak SC, et al. Characterization and prevalence of PITX2 microdeletions and mutations in Axenfeld-Rieger malformations. *Invest Ophthalmol Vis Sci.* 2004;45:828–833.
16. Lehmann OJ, Ebenezer ND, Ekong R, et al. Ocular developmental abnormalities and glaucoma associated with interstitial 6p25 duplications and deletions. *Invest Ophthalmol Vis Sci.* 2002;43:1843–1849.
17. Lehmann OJ, Ebenezer ND, Jordan T, et al. Chromosomal duplication involving the forkhead transcription factor gene FOXC1 causes iris hypoplasia and glaucoma. *Am J Hum Genet.* 2000;67:1129–1135.
18. Berry FB, Lines MA, Oas JM, et al. Functional interactions between FOXC1 and PITX2 underlie the sensitivity to FOXC1 gene dose in Axenfeld-Rieger syndrome and anterior segment dysgenesis. *Hum Mol Genet.* 2006;15:905–919.
19. Tamimi Y, Lines M, Coca-Prados M, Walter MA. Identification of target genes regulated by FOXC1 using nickel agarose-based chromatin enrichment. *Invest Ophthalmol Vis Sci.* 2004;45:3904–3913.
20. Tamimi Y, Skarie JM, Footz T, Berry FB, Link BA, Walter MA. FGF19 is a target for FOXC1 regulation in ciliary body-derived cells. *Hum Mol Genet.* 2006;15:3229–3240.
21. Sommer P, Napier HR, Hogan BL, Kidson SH. Identification of Tgf beta1i4 as a downstream target of Foxc1. *Dev Growth Differ.* 2006;48:297–308.
22. Berry FB, O'Neill MA, Coca-Prados M, Walter MA. FOXC1 transcriptional regulatory activity is impaired by PBX1 in a filamin A-mediated manner. *Mol Cell Biol.* 2005;25:1415–1424.
23. Huang L, Chi J, Berry FB, Footz TK, Sharp MW, Walter MA. Human p32 is a novel FOXC1-interacting protein that regulates FOXC1 transcriptional activity in ocular cells. *Invest Ophthalmol Vis Sci.* 2008;49:5243–5249.
24. Smith RS, Zabaleta A, Kume T, et al. Haploinsufficiency of the transcription factors FOXC1 and FOXC2 results in aberrant ocular development. *Hum Mol Genet.* 2000;9:1021–1032.
25. Cox CJ, Espinoza HM, McWilliams B, et al. Differential regulation of gene expression by PITX2 isoforms. *J Biol Chem.* 2002;277:25001–25010.
26. The UniProt Consortium. The Universal Protein Resource (UniProt). *Nucleic Acids Res.* 2009;37:D169–D174.
27. Hubbard T, Barker D, Birney E, et al. The Ensembl genome database project. *Nucleic Acids Res.* 2002;30:38–41.
28. Schouten JP, McElgunn CJ, Waaijer R, Zwijnenburg D, Diepvens F, Pals G. Relative quantification of 40 nucleic acid sequences by multiplex ligation-dependent probe amplification. *Nucleic Acids Res.* 2002;30:e57.
29. Menten B, Pattyn F, De Preter K, et al. arrayCGHbase: an analysis platform for comparative genomic hybridization microarrays. *BMC Bioinformatics.* 2005;6:124.
30. Buysse K, Delle Chiaie B, Van Coster R, et al. Challenges for CNV interpretation in clinical molecular karyotyping: lessons learned from a 1001 sample experience. *Eur J Med Genet.* 2009;52:398–403.
31. Footz T, Idrees F, Acharya M, Kozlowski K, Walter MA. Analysis of mutations of the PITX2 transcription factor found in patients with Axenfeld-Rieger syndrome. *Invest Ophthalmol Vis Sci.* 2009;50:2599–2606.
32. Perveen R, Lloyd IC, Clayton-Smith J, et al. Phenotypic variability and asymmetry of Rieger syndrome associated with PITX2 mutations. *Invest Ophthalmol Vis Sci.* 2000;41:2456–2460.
33. Honkanen RA, Nishimura DY, Swiderski RE, et al. A family with Axenfeld-Rieger syndrome and Peters Anomaly caused by a point mutation (Phe112Ser) in the FOXC1 gene. *Am J Ophthalmol.* 2003;135:368–375.
34. Suzuki T, Takahashi K, Kuwahara S, Wada Y, Abe T, Tamai M. A novel (Pro79Thr) mutation in the FKHL7 gene in a Japanese family with Axenfeld-Rieger syndrome. *Am J Ophthalmol.* 2001;132:572–575.
35. Aldinger KA, Lehmann OJ, Hudgins L, et al. FOXC1 is required for normal cerebellar development and is a major contributor to chromosome 6p25.3 Dandy-Walker malformation. *Nat Genet.* 2009;41:1037–1042.
36. Vissers LE, Bhatt SS, Janssen IM, et al. Rare pathogenic microdeletions and tandem duplications are microhomology-mediated and stimulated by local genomic architecture. *Hum Mol Genet.* 2009;18:3579–3593.
37. D'haene B, Vandesompele J, Hellemans J. Accurate and objective copy number profiling using real-time quantitative PCR. *Methods.* 2010;50:262–270.
38. Lesnik Oberstein SA, Kriek M, White SJ, et al. Peters Plus syndrome is caused by mutations in B3GALTL, a putative glycosyltransferase. *Am J Hum Genet.* 2006;79:562–566.